International Journal of Nanomedicine

Dovepress

open access to scientific and medical research

Open Access Full Text Article

ORIGINAL RESEARCH

Synthesis of Silver Nanoparticle Employing Corn Cob Xylan as a Reducing Agent with Anti-*Trypanosoma cruzi* Activity

This article was published in the following Dove Press journal:
International Journal of Nanomedicine

Talita Katiane Brito,[1,2,*] Rony Lucas Silva Viana,[2,3,*] Cláudia Jassica Gonçalves Moreno,[3,4] Jefferson da Silva Barbosa,[1,2,5] Francimar Lopes de Sousa Júnior,[6] Mayara Jane Campos de Medeiros,[6] Raniere Fagundes Melo-Silveira,[2,3] Jailma Almeida-Lima,[1–3] Daniel de Lima Pontes,[6] Marcelo Sousa Silva,[3,4,7] Hugo Alexandre Oliveira Rocha[1–3]

[1]Postgraduate Program in Health Sciences, Federal University of Rio Grande do Norte (UFRN), Natal, Rio Grande do Norte 59012-570, Brazil; [2]Laboratory of Biotechnology of Natural Polymers (BIOPOL), Department of Biochemistry, Center of Biosciences, Federal University of Rio Grande do Norte (UFRN), Natal, Rio Grande do Norte 59078-970, Brazil; [3]Postgraduate Program in Biochemistry, Federal University of Rio Grande do Norte UFRN), Natal, Rio Grande do Norte 59078-970, Brazil; [4]Laboratory of Immunoparasitology, Department of Clinical and Toxicological Analysis, Health Sciences Center, Federal University of Rio Grande do Norte, Natal, Rio Grande do Norte 59012-570, Brazil; [5]Federal Institute of Education, Science and Technology of Rio Grande do Norte (IFRN), Natal, Rio Grande do Norte 59500-000, Brazil; [6]Laboratory of Chemistry of Coordination and Polymers (LQCPol), Institute of Chemistry, Federal University of Rio Grande do Norte (UFRN), Natal, Rio Grande do Norte 59078-970, Brazil; [7]Global Health and Tropical Medicine, Institute of Hygiene and Tropical Medicine, New University of Lisbon, Lisboa 1349-008, Portugal

*These authors contributed equally to this work

Correspondence: Hugo Alexandre Oliveira Rocha
Laboratory of Biotechnology of Natural Polymers (BIOPOL), Department of Biochemistry, Center of Biosciences, Federal University of Rio Grande do Norte (UFRN), Natal, Rio Grande do Norte 59078-970, Brazil
Email hugo@cb.ufrn.br

Background: Chagas disease, also known as American Trypanosomiasis, is caused by the protozoan *Trypanosoma cruzi*. It is occurring in Americas, including USA and Canada, and Europe and its current treatment involves the use of two drugs as follows: benznidazole (BNZ) and nifurtimox, which present high toxicity and low efficacy during the chronic phase of the disease, thus promoting the search for more effective therapeutic alternatives. Amongst them xylan, a bioactive polysaccharide, extracted from corn cob.

Methods: Ultraviolet-visible spectroscopy, Fourier transform infrared spectroscopy (FITR), Raman spectroscopy, energy-dispersive X-ray spectroscopy (EDS), scanning electron microscopy, atomic force microscopy, plasma optical emission spectroscopy (ICP-OES), dynamic light scattering (DLS) have been used to characterize the silver-xylan nanoparticles (NX). Their cytotoxicity was evaluated with 3-bromo(4,5-dimethylthiazol-2-yl)-2,5-diphenyltetrazolium (MTT) test. MTT and flow cytometry were used to ascertain the anti-*Trypanosoma cruzi* activity.

Results: UV-Vis spectroscopy gave plasmon resonance ranging between 400 and 450 nm while FITC and Raman spectroscopy proved nano interface functionalized with xylan. ICP-OES data showed NX with xylan (81%) and silver (19%). EDS showed NX consisting of carbon (59.4%), oxygen (26.2%) and silver (4.8%) main elements. Spherical NX of 55 nm average size has been depicted with SEM and AFM, while DLS showed 102 ± 1.7 nm NX. The NX displayed negligible cytotoxicity (2000 µg/mL). NX (100 µg/mL) was more effective, regardless of experiment time, in affecting the ability of parasites to reduce MTT than BZN (100 µg/mL). In addition, NX (100 µg/mL) induced death of 95% of parasites by necrosis.

Conclusion: This is the first time silver nanoparticles are presented as an anti-*Trypanosoma cruzi* agent and the data point to the potential application of NX to new preclinical studies in vitro and in vivo.

Keywords: xylan, silver nanoparticles, *Trypanosoma cruzi*, benznidazole

Introduction

For several years, Chagas disease had assumed a predominantly rural profile, but has now become part of the urban zone due to movement of the population from country sides to cities, due to increased deforestation and socioeconomic changes. This migration has also affected non-endemic areas such as Europe, the USA and Canada.[1–3] Also known as American Trypanosomiasis, it is caused by the protozoan *Trypanosoma cruzi* and is transmitted among other forms by insects of the *Triatominae* subfamilies.[4] It is estimated that around 8 million people worldwide, particularly those residing in Latin America, are infected with *T. cruzi*. More than

10 thousand people die of the disease every year and more than 25 million are at a risk of acquiring it.[5]

Chagas disease has two successive phases, acute and chronic.[2] There are no vaccines to treat the patients affected by the disease and their treatment is pharmacological. On the other hand, these drugs are used to treat the disease mainly in its acute phase, reducing symptoms and parasitemia. The current treatment involves the use of two drugs: benznidazole (BNZ) and nifurtimox. Both are far from ideal due to their side effects, limited efficacy and little is known about their activity in the chronic phase. These disadvantages justify the urgent need to identify better drugs for the treatment of chagasic patients.[6,7] Considering this scenario, researches aimed at prospecting bioactive molecules from natural sources have increased significantly over the years.[8–11]

In the secondary cell walls of Gramineae and dicotyledons, for example, the main hemicellulose is a polymer composed of D-xylose units linked by β glycosidic (1 → 4) bonds called xylans.[12] Xylans from different sources have been used in the biosynthesis of grafts, bandages and sutures, synthesis of micro and nanoparticles[13,14] as well as for the controlled release of drugs.[15–17] It has been reported in the literature that corn cobs (Gramineae), underutilized in industry and often discarded, are the most promising material for the extraction of these biopolymers.[18]

It has been documented that xylans obtained from corn cobs had a chemical composition consisting of 4-O-methyl-D-glucuronic acid, L-arabinose and D-xylose in a ratio of 2:7:19.[19,20] It has been also reported that the xylans from corn cobs demonstrate immunomodulatory,[21] antioxidant, anticoagulant and antibacterial properties as well as cytotoxicity to tumor cells.[22]

Several papers have demonstrated nanomaterials acting as toxic agents against various types of parasites. However, there are few studies regarding *T. cruzi*. The antichagasic activity of sesquiterpene lychnopholide (LYC) loaded into polymeric nanocapsules (NCs), thiol capped quantum dots, and a nanoparticle (~37 nm) containing actinomycin D and a cholesterol-vinyl sulfone compound bound to Staphylococcal protein A covalently and coated with anti-*Trypanosoma cruzi* IgG were tested.[23] Regarding metal containing nanoparticles, studies were performed with silver and gold nanoparticles. However, they had been performed with *Trypanosoma brucei*.[24,25] On the other hand, there are no papers that have evaluated the action of these nanoparticles against *T. cruzi.*

Several methods of nanoparticle synthesis, including silver nanoparticles, often lead to the production of several undesirable wastes which are harmful to the environment. Therefore, the search for more effective and environmentally friendly methods is ongoing. These methods are known as green synthetic methods and are considered efficient since they do not use toxic reagents, such as water, for the environment.[26]

Studies from our research group have shown that the green synthesis of silver nanoparticles with polysaccharides has potentiated the biological activity of both polysaccharides and silver. According to Amorim et al,[27] the cytotoxic activity of sulfated polysaccharides (sPS) of the seaweed *Spatoglossum schröederi* was potentiated against renal adenocarcinoma cells 786–0. Also, the antitumor, immunomodulatory and antibacterial activities of the sPS of the seaweed *Dictyota mertensii* had intensified.[28] In both cases, they composed the structure of silver nanoparticles.

It has been previously demonstrated by our research group that xylan from corn cobs exhibits several biological activities, particularly, antiproliferative activity against uterine adenocarcinoma cells[29] and antioxidant activity.[22] However, the activities of this molecule were not evaluated when they are part of the silver nanoparticle structure regarding its antiparasitic activity against *T. cruzi*. Therefore, in this present study, biosynthesized silver nanoparticles from corn cobs containing xylans were tested/evaluated against *T. cruzi.*

Materials and Methods

Materials

MTT (3-bromo-(4,5-dimethylthiazol-2-yl)-2,5-diphenyltetrazolium), silver nitrate ($AgNO_3$), D-xylose, bovine serum albumin (BSA), cell culture media – liver infusion tryptose (LIT), dextrose, hemina, tryptose and liver infusion broth were purchased from the Sigma Chemical Company (St. Louis, MO, USA). NaCl, KCl and Na_2HPO_4 from the INLAB (São Paulo, SP, Brazil). Sterile fetal bovine serum was purchased from the Cultilab (Campinas, SP, Brazil). Benznidazole (Rochagan) Hoffmann-La Roche (Basel, Switzerland) was provided by the consortium of the BERENICE project whose name was built from letters that make up the name of the consortium (**BE**nznidazole and Triazole **RE**search group for **N**anomedicine and **I**nnovation on **C**hagas diseas**E** - Barcelona, Spain). We also procured the Bradford reagent from the Bio-Rad Laboratories, Inc.

(Hercules, CA, USA) and the Folin-Ciocalteau reagent and dimethyl sulfoxide (SDS) from the Merck KGaA (Darmstadt, Hessen, Germany). Penicillin and streptomycin were obtained from Thermo Fisher Scientific (Waltham, Massachusetts, USA). Sodium hydroxide, sulfuric acid and methanol were purchased from the CRQ (Diadema, SP, Brazil). Phenol was obtained from the Reagen Quimibrás Indústrias Químicas S. A. (Rio de Janeiro, RJ, Brazil). Annexin V Apoptosis Detection Kit for flow cytometry (Annexin-FITC, Propionate Iodide – PercP) was purchased from BD Biosciences Inc. (San Diego, CA, USA).

Extraction of Xylan from Corn Cobs

Fresh corn samples bought from a local market (Natal, RN – Brazil) were peeled, cleaned and washed. They were then cut into small pieces, dried in a kiln at 60°C under ventilation and ground until its flour was obtained. 160 mL of methanol was added to 10 g of flour produced from the cob and the material was stirred for 24 hrs in the dark to remove lipids and pigments. The precipitate was collected by centrifugation (10,000 × g, 20 min, 4°C), dried and stored in hermetically sealed vials at 25°C until use. For the extraction of the polysaccharides, 25 mL of the solution of NaOH (1.8 mol/L) in the ratio of 1:25 (w/v) was added to 1 g of corn cob flour. This solution was sonicated at an ultrasound power of 200 W for 30 mins at intervals of 5 mins and a temperature of 60°C. The solution was centrifuged to separate the extracted material from the insoluble residue. Four volumes of chilled methanol were added to the supernatant under conditions of gentle agitation and was held protected from light at 4°C for 24 hrs. The precipitate thus formed was collected by centrifugation (10,000 × g, 20 min, 4°C), dried and stored in flasks at 25°C for further analysis.

Chemical Analysis of Xylan

Folin-Ciocalteau[30] and Bradford[31] methods were used to rule out the presence of phenolic compounds and proteins in the xylan sample, respectively. Gallic acid and bovine albumin were used as the standard, respectively, for each method. Total sugars were analyzed by the reaction of phenol-H_2SO_4 and D-xylose was used as the standard.[32]

Determination of the Monosaccharide Composition of Xylan

An analysis of the monosaccharide composition was performed as described by Melo-Silveira et al[22] The material after being hydrolysed was subjected to sugar composition analysis using the LaChrom Elite® VWR-Hitachi high performance liquid chromatography (HPLC) system with a L-2490 refractive index detector. The column used was LichroCART® 250–4 Lichrospher® 100 NH_2 (10 µM). The mobile phase used in the test was with acetonitrile: water (80:20) in a flow rate of 1 mL/min, at 40°C. The following sugars were analysed as references: arabinose, galactose, glucose, glucuronic acid, fructose, fucose, mannose, N-acetyl-glucosamine, galactosamine, rhamnose and xylose.

Synthesis of Nano Xylans Silver

The nano xylans were obtained using the process of green synthesis as described by Dipankar and Murugan[33] The corn cob xylan was used as a bioreductor in this experiment. The synthesis of NX was performed by the addition of a solution of 1.0 mM silver nitrate to a 10 mg/mL (1:9 w/v) solution of xylan. The solution was subjected to continuous stirring for 24 hrs and was placed in conditions protected from the light. After this period, it was centrifuged at 10,000 × g for 15 mins at 25°C. The precipitate was collected and lyophilized.

Characterization of the Nanoparticles

UV-Visible Spectroscopy

The formation of NX and reduction of silver were analysed by observing a change in the colour (from light yellow to dark brown) of the solution. Electron spectroscopy in the UV-visible region with readings in the 350 to 800 nm range was performed to monitor these reactions using the UV/Visible spectrophotometer model DR 5000 Hach Lange GmbH (Düsseldorf, Germany).

Atomic Force Microscopy (AFM), Energy Dispersive X-Ray Spectroscopy (EDS), Dynamic Light Scattering (DLS), and Scanning Electron microscopy (SEM) Analysis

Atomic force microscopy (AFM) and energy-dispersive X-ray spectroscopy (EDS) were performed by a Scanning Probe Microscope (SPM) 9700 (Shimadzu, Kyoto, Japan) and a Scanning Electron Microscope TM-3000 (Hitachi, Kyoto, Japan), respectively, at the Scanning Electron Microscopy Laboratory (LABMEV), in the Department of Engineering Materials (DEMat), of Universidade Federal do Rio Grande do Norte (UFRN). At least three images were taken in different fields. All images were evaluated for the shape of the samples.

One drop of the NX suspension (0.5 mg/mL) was dried on a glass cover slip and submitted to AFM analysis. EDS

analyses were made with dry NX that was dropped onto carbon tape.

NX was also analyzed by dynamic light scattering and SEM. The hydrodynamic diameter, polydispersity index (PDI), and zeta potential were determined on a Zeta Potential Analyzer (Brookhaven, New York, NY, USA). Briefly, NX suspensions (0.5 mg/mL) were analyzed in three independent experiments, and the reported values correspond to mean ± SD.

NX was processed and analyzed by SEM (Shimadzu electron microscope, model SSX550; Shimadzu Corp., Kyoto, Japan) analysis. Briefly, 20 µL of NX (0.5 mg/mL) sample was loaded on carbon-coated copper grid without gold coating and air-dried for 10 mins under vacuum. The grid chamber was placed in the SEM room and incubated in the dark at 10–20°C for 2 hrs. Finally, the grid chamber was loaded on the TEM stage for analysis and images were captured from different zones with different resolution. Representative image of three independent experiments is shown.

Quantitative Determination of Silver in Nano Xylans by Coupled Plasma Optical Emission Spectroscopy (ICP-OES)

NX Digestion

Analytical scales were used to weigh 100 mg of sample in Teflon cups (total 200 mg of sample; 100 mg of each cup), to which 7 mL of 65% nitric acid purified by sub-boiling distillation (Berghof, Eningen, Germany) and 1mL of 30% hydrogen peroxide (Merck, Darmstadt, Germany) were added. The digestion cups were subsequently closed and digestion was performed in a microwave digester (Start D, Milestone, Italy) using 6 stages and a power of 1100W:(1) 5 mins at 70°C; (2) 2 mins at 70°C; (3) 3 mins at 120°C; (4) 2 mins at 120°C;(5) 10 mins at 170°C; (6) 15 mins at 170°C and lastly 30 mins of ventilation before there modal of the rotor from the microwave. The digested content was quantitatively made up to 15 mL using deionized water and filtered through a 0.45 µm membrane. The analyses were conducted in duplicate and analytical blanks were performed by conducting the procedure in the absence of sample.

Determination of Silver Content the Digested NX

Silver content of digested NX was quantified using an inductively coupled plasma emission spectrometer (ICP-OES 5100 VDV, Agilent Technologies, Tokyo, Japan) in axial view, equipped with a radio frequency source (RF) of 27 MHz, using a simultaneous optical detector, a peristaltic pump, a double pass cyclonic spray chamber, a 1.8 mm quartz torch, and a spray glass nebulizer. The gas used in the system was plasma liquid argon with a purity of 99.996% (White Martins, SP, Brazil). The ICP-OES equipment operated under the following conditions: power of the plasma, 1.5 kW; argon flow, 12.0 L/min; auxiliary argon flow, 1.0 L/min; nebulization flow, 0.70 L/min; number of replicates, 3; stabilization and reading time, 15 s, wavelength, 328.068 nm. The analytical curve for silver was prepared by diluting 1000 mg/L of reference standard solution (Merck, Darmstadt, Germany) into a 2.5–100 g/L range (r= 0.9999) in a solution of 5% (v/v) nitric acid prepared from 65% acid distilled in a sub-boiling system (Distillacid, Berghof, Eningen, Germany). Serial dilutions were prepared for sample measurement: i) 0.1 mL/10 mL and ii) 0.2 mL/10 mL.

Fourier-Transform Infrared Spectroscopy (FT-IR)

The samples (10 mg) were mixed with KBr, triturated, and pellets, made from this material were subjected to FT-IR. Spectra of the samples were obtained using a spectrophotometer (IRAAffinity-1 Shimadzu Corp., Kyoto, Japan) equipped with the IRsolution Shimadzu Corp. software (Kyoto, Japan) version 1.60 with scan number 32 and 4 cm^{-1} resolution. The frequency range for the analysis was 4000 to 400 cm^{-1}. The analyses were carried out at the analytical center of UFRN's Chemistry Institute and the Coordination and Polymers Chemistry Laboratory (Laboratório de Química de Coordenação e Polímeros - LQCPol – Department of Chemistry) of the Federal University of Rio Grande do Norte (Universidade Federal do Rio Grande do Norte – UFRN). Three independent analyses were performed.

Analysis Using Raman Spectroscopy

The Raman spectra were obtained from pre-crushed samples in the solid state. The samples were analysed using the Raman confocal microscope, model LabRAM HR Evolution, HORIBA Scientific with the CCD detector. For this purpose, the 633 nm laser with an acquisition time of 20 s and 2 s of accumulation in the region of 30 to 4000 cm^{-1} was used. The analyses were carried out at the Coordination and Polymers Chemistry Laboratory (Laboratório de Química de Coordenação e Polímeros – LQCPol – Department of Chemistry) of the Federal University of Rio Grande do Norte (Universidade Federal do Rio Grande do Norte – UFRN).

The Cytotoxicity Activity of NX

The cytotoxicity activity of NX was evaluated in vitro using MTT test. Murine macrophage cell line (RAW 264.7 ATCC TIB-71) and mouse fibroblast (3T3 ATCC CCL-92) were cultivated in Dulbecco's modified eagle medium (DMEM) supplemented with 10% fetal bovine serum (FBS). Briefly, $5x10^3$ cells/well were plated in a 96-well plate. After 24 hrs incubation (95% air, 5% CO_2, 37°C), the medium was replaced by a DMEM without FBS, followed by incubation for another 24 hrs in order to stimulate cells to enter in G0 phase. The medium was replaced by a DMEM with 10% FBS added to NX at concentrations 0.01, 0.025, 0.050, 0.1, 0.25, 0.5, 0.75 or 1.0 mg/mL. At the end of incubation period (24 hrs), the medium was replaced by a new DMEM without FBS added to 1.0 mg/mL of 3-(4,5-dimethylthiazol-2-yl)-2,5-diphenyltetrazolium bromide (MTT), followed by incubation for 4 hrs at 37°C. The medium was removed, and formazan crystals were dissolved with 100 µL of 95% ethanol. After 15 mins shaking in a rocking shaker, absorbance was read (570 nm) in a microplate spectrophotometer (Biotek, Winooski, Vermont, USA). As a negative control, cells were cultivated only with DMEM with 10% FBS. Results were expressed in the percentage of MTT reduction, as in Equation 1.

$$\text{Percentage MTT Reduction} = (\text{Absorbance of sample} / \text{Absorbance of control}) \times 100 \quad (1)$$

Evaluation of the Antiparasitic Activity of Nano Xylan by the Colorimetric MTT (3-Bromo(4,5-Dimethylthiazol-2-Yl)-2,5-Diphenyltetrazolium) Reduction Assay

The epimastigote forms of the Y strain of *T. cruzi* were maintained in LIT supplemented with 10% fetal bovine serum (FBS) from Thermo Fisher Scientific (Waltham, MA – USA) at 28 ± 2°C in a biochemical oxygen demand (BOD) kiln. The strains were cultured until the exponential phase of growth (1×10^7 parasites/mL) was reached. Samples were tested at concentrations of 2.5, 10 and 100 µg/mL. Therefore, 90 µL of the culture (1×10^7 parasites) and 10 µL of nanoparticles suspension (10 mg/mL, 1 mg/mL or 0.25 mg/mL) were added to a 96-well plate and incubated at 28 ± 2°C for 24 hrs and 48 hrs. After incubation, 10 µL of MTT (5 mg) was added, and after 75 mins of incubation in a BOD kiln, 100 µL of the solubilisation solution (0.01N HCl and 10% SDS) was added. Absorbance was read at 570 nm using the Epoch Microplate Spectrophotometer obtained from BioTek (Winooski, VT, USA). The assays were performed in triplicate and the data obtained were processed with the GraphPad Prism software version 5.0, 2014 (La Jolla, California, USA).

Flow Cytometry

The mechanisms of cell death of the *T. cruzi* parasite through apoptosis/necrosis were investigated by labelling with Annexin V-FITC (fluorescein isothiocyanate)/Propidium iodide (PI) by following the manufacturer's instructions from the Annexin V FITC Apoptosis Detection Kit – Invitrogen. The epimastigote forms of the Y strain of *T. cruzi* (1×10^7 cells/mL) were cultured in LIT supplemented with 10% FBS were treated with NX (0.25, 1, and 100 µg/mL) for 24 hrs. After the parasites were centrifuged at a speed of 2000 rpm at 4°C for 5 mins. The pellet, thus obtained, was washed with phosphate-buffered saline (PBS), resuspended in the binding buffer and the Annexin V/PI labeling was performed for 10 mins at 25°C protected from the light. The analysis was performed on the FACSCanto II flow cytometer (BD Biosciences, Eugene, OR, USA) with the FACSDiva software, version 6.1.2 (Becton Dickson, Franklin Lakes, NJ, USA). For each experimental condition, 20,000 events were captured, and the percentage of labeled cells was calculated in the FlowJo Software Version vX.0.7 1997–2014 (FlowJo, Ashland, OR, USA).

Statistical Analysis

The experiments were performed at least twice and in triplicates. Data were analysed using the ANOVA test, followed by the Tukey's test. Statistical analyses were conducted using the Prism 5 software (GraphPad software, version 5.0, 2014 La Jolla, California, USA). Values of $p < 0.05$ were considered statistically significant. The results were expressed as mean ± standard deviation.

Results and Discussion

Extraction and Chemical Analysis of the Corn Cob Xylan

Xylan was extracted as described in the Methods section, and the content of total sugars, proteins and phenolic compounds was determined in the extracted xylan. It can be observed in Table 1 that the sample consists majorly of carbohydrates (97.42%), and the obtained xylan is composed mainly of xylose (50%), glucose (20%), arabinose (15%) and galactose (10%) as well as some amounts of

Table 1 Chemical Composition of Xylan Extracted from Corn Cob

Sample	Polysaccharide (%)	Protein (%)	Phenolic Compounds (%)	Molar Ratio (%)					
				Xyl	Glc	Ara	Gal	Man	GlcA
Xylan	97.42	2.18	0.40	50.0	20.0	15.0	10.0	2.5	2.5

Abbreviations: xyl, xylose; ara, arabinose; glc, glucose; gal, galactose; man, mannose; GlcA, glucuronic acid.

mannose (2.5%) and glucuronic acid (2.5%) residues. Similar compositions of monosaccharides were observed in other studies that evaluated xylans extracted from corn cob[34] although their values differed from those observed in our work. On the other hand, in the corn cob xylan studied by Melo-Silveira et al[22,26] the composition of monosaccharides as well as their proportions were similar to those presented in Table 1. It is worth mentioning that these authors used the same process described in this study.

Synthesis of Silver Nanoparticles with Xylan (Nano Xylan)

The UV-Vis spectroscopy was used as an essential tool to confirm the synthesis of nanoparticles containing silver[30] and assist in the analysis for the formation of nanocomposites with reduced silver. Therefore, an analysis was performed using this technique with a scanning range of 350–800 nm for the silver nanoparticle solution. In the region highlighted by the rectangle (between 400–450 nm) in Figure 1, a change in the light absorption profile, evidenced by a small increase in the absorbance values, is observed. From this region, a decrease in the absorbance is observed that almost reaches zero during the sweep. When the silver nitrate or xylan solutions were analysed separately in the 400–450 nm range, the same light absorption profile was not observed in this wavelength range (data not shown). This signal is characteristic of reduced silver and indicates the formation of silver nanoparticles.[35,36] Similar to the use of xylan employed in this work, in other studies, the use of polysaccharides with reducing agents to synthesize silver nanoparticles has already been described.[27,28,37]

Determination of the Composition of NX

Constituents of NX were determined using an inductively coupled plasma emission spectrometer as described in the Methods section and were found to consist of xylan (81%) and silver (19%). There are no reports in the literature about studies that have evaluated the amount of silver in

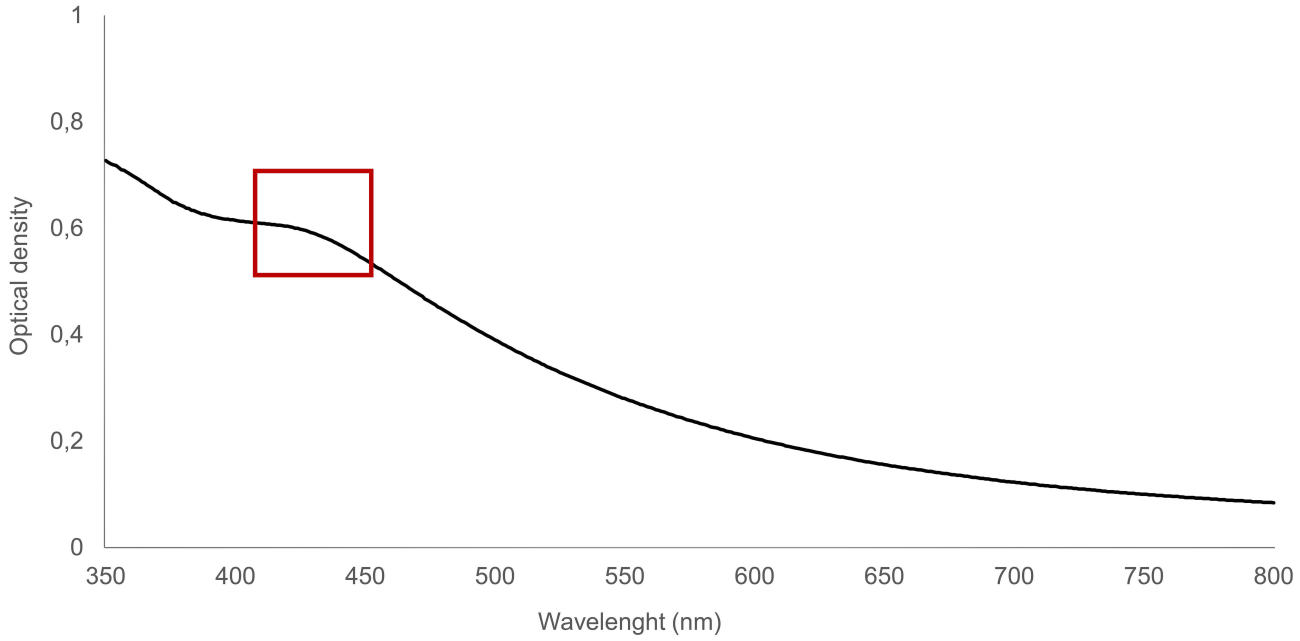

Figure 1 UV-visible light absorption spectrum of the silver nanoparticle suspension. Scan performed between 350 and 800 nm.

nanoparticles synthesized with the xylan polysaccharide. However, some authors have verified the amount of silver in the structure of nanoparticles containing other polysaccharides. In studies conducted by Amorim et al[27] and Chen et al,[38] 7% and 6.7% of silver were found, respectively, in a fucan-coated nanoparticle composition and in nanoparticles synthesized with fungal exopolysaccharide. These values are lower than those obtained by us in our study using corn cob xylans. However, it is worth mentioning that the efficiency of synthesis of silver nanoparticles and their characteristics depend on certain factors such as temperature, concentration of plant extract used during the process and reaction time,[39] which would explain the previously described variation in values as well as the variation presented in this study.

Characterization of NX

SEM image of NX providing information on the morphology and size of the nanoparticles is shown in Figure 2A and B. The particles were predominantly spherical in shape, aggregated and have an average size of 55.3 ± 10 nm. NX average size was also determined using AFM, which was approximately 40 nm. In addition, AFM also showed NX with a rounded/spherical shape (Figure 2C and D). The mean volume hydrodynamic size of particles in water as measured by DLS was 102.3 ± 1.7 nm (Figure 2E).

The size of the NX as determined by SEM is much smaller compared to the DLS measurements, which is expected as DLS measures the hydrodynamic radius of the nanoparticles suspended in water together with any coating material on the surface of the nanoparticle.[40] The difference in size for the SEM/AFM and DLS data can therefore be assumed to be due to the capping agent present on the NX surface, i.e., the xylan.

NX has polydispersity index (PDI) value of 0.178. A PDI index of less than 0.1 represents monodispersed NPs, while an index of between 0.1 ≤ 0.2 indicates a narrow size distribution, while an index between 0.2 ≤ 0.5 indicates a broad size distribution for the sample.[41]

It is possible to obtain nanoparticles larger or smaller than those found in this research. However, silver nanoparticles with sizes ranging from 5 to 150 nm in diameter[42–45] have been commonly observed in literature. Another

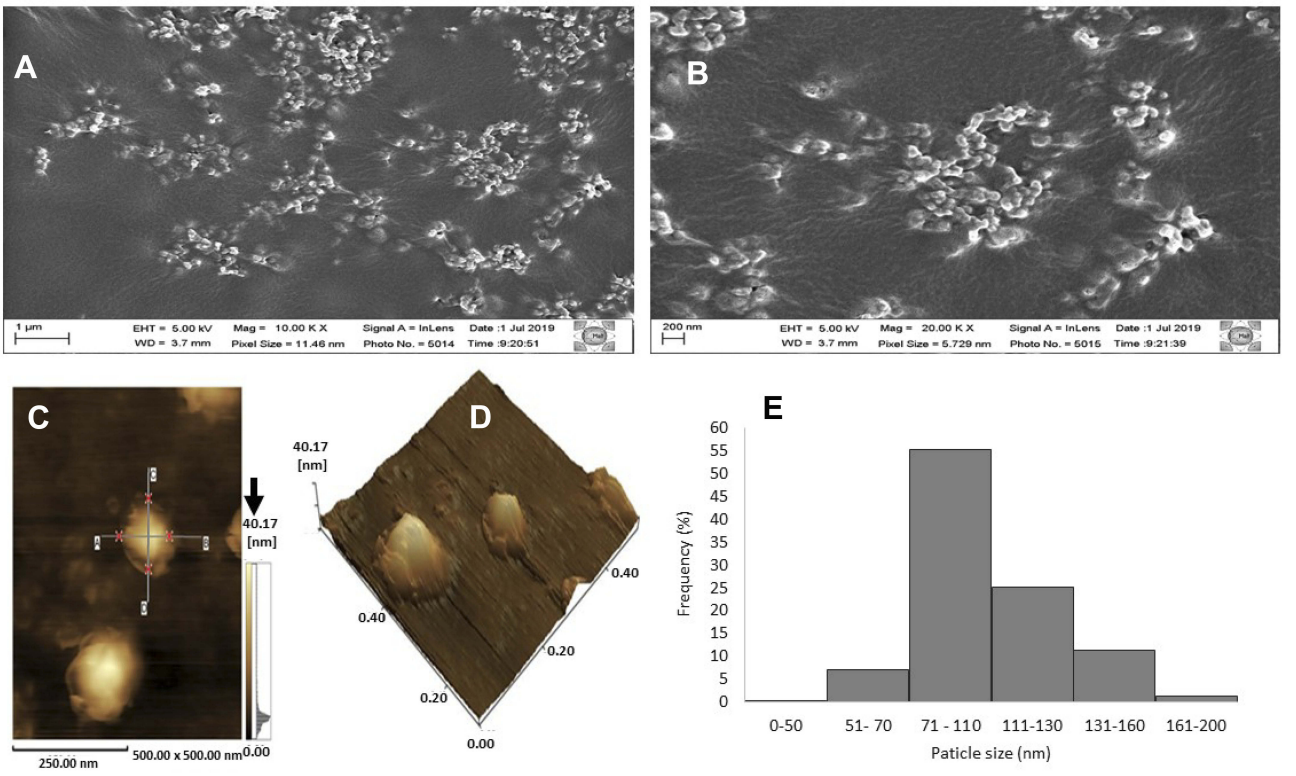

Figure 2 (**A** and **B**) Appearance of NX identified by scanning electron microscopy (SEM). Atomic Force Microscopy of silver nanoparticles containing corn cob xylan. In (**C**) the nanoparticle can be seen in two dimensions. The arrow indicates the size of the nanoparticle (40.17 nm). (**D**) shows the representation of image C in three dimensions. It is also possible to observe the rounded shape of the particles. (**E**) Size dispersion histogram obtained by dynamic light scattering (DLS).

essential characteristic is the relation between the size of the nanoparticles and the response they cause in biological systems, since the cytotoxicity of silver nanoparticles is influenced by variations in their particle size.[42]

Studies report that smaller particles can induce higher cytotoxicity since they can be easily internalized by the cells. To support this hypothesis, Carlson et al[43] using silver nanoparticles of sizes 15, 30 and 55 nm, found that the smaller nanoparticles (15 nm) generated more reactive oxygen species in murine macrophage lines. Liu et al[44] in turn, working with four human cell lines (A549, HepG2, MCF-7 and SGC-7901), also found that silver nanoparticles with a diameter of 5 nm were more toxic than those with 20 and 50 nm.

Morphology is another factor that can influence the activity of different types of silver nanoparticles. The most commonly produced structures are as follows: spherical, triangular, square, cubic, rectangular, oval and acicular. Considering their toxicity, it is not yet known which form of the particle has the best effect on biological systems and it will depend on several factors (concentration, pH, temperature, electric charge) instead of a single factor. However, what has already been observed is that spherical-shaped silver nanoparticles, such as the NX studied in this work, do not have damaging effects on the cells.[45,46]

Zeta potential analysis revealed that NX has a surface charge of - 13.4 ± 3.6 mV. Energy-dispersive X-ray spectroscopy (EDS) analysis (Table 2 and Figure 3) indicated the elements on the surface of the sample. Oxygen, carbon, sodium and silver were the main elements. The peaks observed at 0.18 and 3.0 keV correspond to the binding energies of silver. As the particles were coated with gold for EDS analysis a peak situated at the binding energy of 2.75 keV belonging to Au has been observed. No peaks of other impurities have been detected, indicating that the silver nanoparticles sample contain pure silver, with no oxide.

Analysis Using FT-IR

FT-IR is an important and widely used technique to study the physicochemical and conformational properties of compounds.[47] Therefore, corn cob xylan and NX were analysed using infrared spectroscopy and its spectra are presented in Figure 4. There was no overlap in the spectra but there is a coincidence of bands found in both.

Table 2 Energy Dispersive X-Ray Spectroscopy Elemental Composition of Synthesized Nanoxylan

	Oxygen (%)	Carbon (%)	Sodium (%)	Silver (%)
Nanoxylan	26.21	59.41	9.54	4.84

Bands in both spectra with absorption close to the 3430.70–3429.93 cm^{-1} regions were attributed to the O-H stretch of the xylan monosaccharides. Oliveira et al[20] reported that this absorption bandwidth occurs because of the stretching of the monosaccharide hydroxyls associated with the water molecules by intra and intermolecular hydrogen bonds.

The presence of arabinose side chains is characterized by a low-intensity band in the 1161.41 cm^{-1} region. This band corresponds to the C–O–C vibrations in the anomeric region of the xylan.[48] Another prominent band observed in the 1046.59 cm^{-1} region of both spectra, which is a characteristic of xylans, was attributed to the stretching of the C-C and C-O groups present in the sugar residues.[49]

The two bands that need to be highlighted are those observed at 896.90 cm^{-1} and 1039.63 cm^{-1}. The first band was attributed to the anomeric carbon of the β-glycosidic bonds of the monosaccharides, while the second band is characteristic of xylans containing β (1→ 4) glycosidic bonds.[50] Also, C, Li[51] and Nacos et al[52] have stated that these bands are characteristics of polysaccharides with xylose units in their main chain.

In both spectra, bands of moderate intensity in the 2936.63 cm^{-1} region were also observed which are characteristic of the C-H group stretches typical of monosaccharides.[53,54]

It has been reported in the literature that bands near the 1400 cm^{-1} region of the nanoparticle spectra correspond to those of reduced silver.[55] With xylan, this band appears in the spectrum of the silver nanoparticles around 1392 cm^{-1}.

We also observed the presence of a band in the 1923 cm^{-1} region of the NX spectrum and its absence in the xylan spectrum, which can be an indicator of the presence of clusters during the formation of the nanoparticle or the superposition of vibrational movements. However, we did not find data in literature reporting the presence of this band in the spectra of the silver nanoparticle with xylan.

Some xylan bands appeared to be displaced in the NX spectra compared to those of the free xylan spectrum, probably because of interaction between the silver and polysaccharide, resulting in modifications in the electron density around the xylan groups and displacing their vibrational modes.

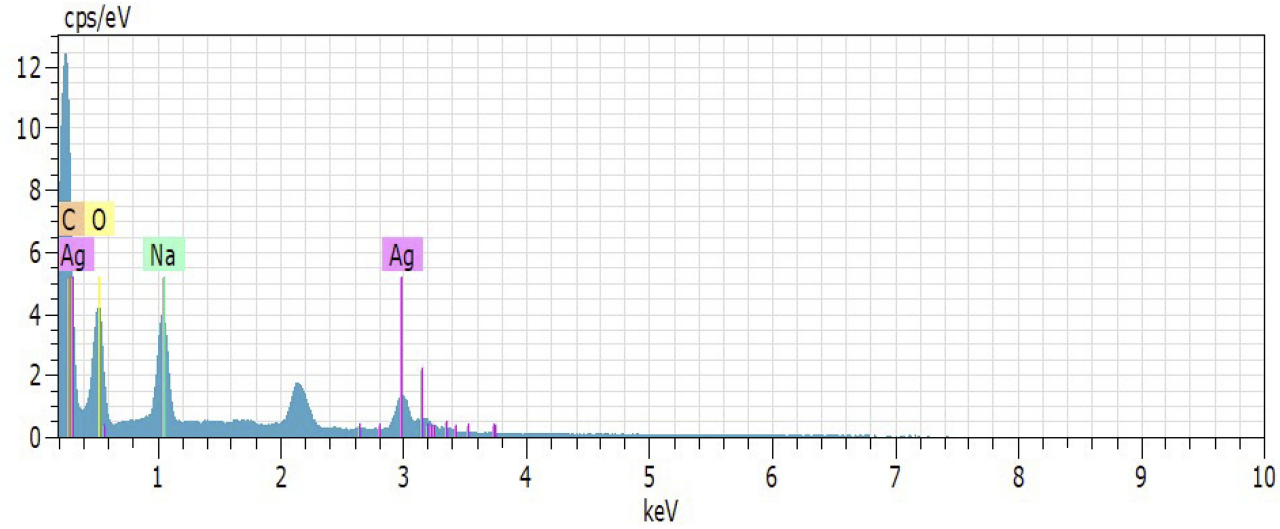

Figure 3 Energy-dispersive X-ray spectroscopy (EDS) analysis.

Infrared analyses suggest the interaction of polysaccharide (xylan) groups with silver, confirming the formation of silver nanoparticles with the corn cob xylan.

Analysis of Xylan and NX Using Raman Spectroscopy

Raman spectroscopy is a technique widely used to complement the study of infrared spectroscopy.[56] This analysis was carried out to confirm the structure of xylan due to its complex nature[57] and to analyse the formation of silver nanoparticles bound to this compound.

There are few reports in literature on the analysis of the structure of xylan using the Raman technique. Therefore, the assignment of bands in the present work was based on interpretations of the spectra and performed using the data obtained from the Raman analyses of other polysaccharides.

In Figure 4, the presence of β-type glycosidic bonds (1→4) is identified by a band common to both spectra in the region around 840.18 cm^{-1}.[58] These authors also evidenced the same band in the Raman spectra of wheat arabinoxylans, which have xylans in its main chain.

Three bands around 1187 cm^{-1} (xylan) and 1201.80 cm^{-1} (NX) can be reported in Figure 5. These bands are closely related to the C-O-H and C-H groups. Zeng et al[57] reported that xylans from the cell walls, that are solubilized by enzymes, also showed bands around the region between 1100 and 1220 cm^{-1}.

Bands of glucopyranose rings were observed in the spectral range of 1100 to 900 cm^{-1}, which are indicative of the C–C and C–O stretch modes.[59]

In the spectrum of NX, it can be noted that the main vibrational modes of xylan, as discussed already, are present and the majority of them have coincident bands except for an intense and wide band in the region of 2721.86 cm^{-1}. However, after analysing many studies that have used the Raman technique to evaluate nanoparticles containing silver and polysaccharides, it was found that none presented an interpretation of this band making it difficult to understand its significance in the NX spectrum. Thus, it is necessary to conduct a study that goes beyond the scope of our work to explain its meaning.

Moreover, this spectrum is clearer and contains bands that are better defined than that of xylan. This corroborates with the report of Li et al,[60] which asserts that the quality of Raman signals is affected by the size of their metal cores.

Data presented in this paper confirm the interaction of xylan with silver and the formation of silver nanoparticles. The synthesis of silver nanoparticles containing polysaccharides aims to improve biological activities not only of the polysaccharides themselves but also of the silver, since the presence of polysaccharides, such as xylan, allows a better acceptance of the nanoparticles by the cells. For example, in the study conducted by Akmaz et al,[61] it was noted that the chitosan/silver nanoparticles had significantly higher bacterial activity than that of pure chitosan.

Evaluation of the Antiparasitic Activity of Nano Xylan by the Colorimetric MTT (3-Bromo(4,5-Dimethylthiazol-2-Yl)-2,5-Diphenyltetrazolium) Reduction Assay

Chagas disease, caused by the protozoan *T. cruzi*, is endemic in Latin America and manifests itself in two distinct

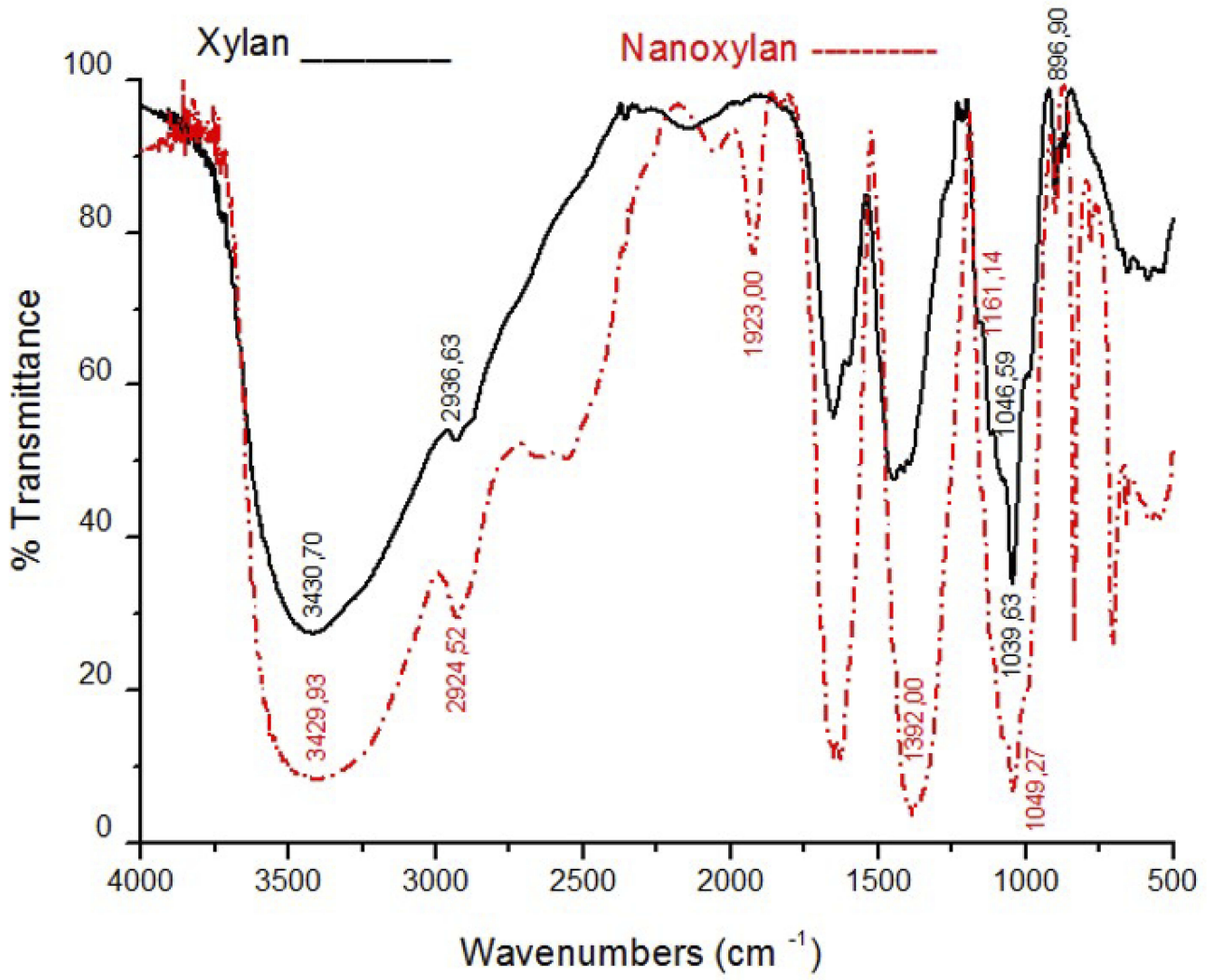

Figure 4 Infrared spectra of corn cob xylan and nano xylan in the 4000 to 500 cm^{-1} regions.

phases, acute and chronic. BNZ is the drug of choice for treatment in the acute phase. However, despite its effectiveness, it is highly toxic. On the other hand, for the chronic phase of the disease, currently, no effective treatment is available. BNZ has low solubility/bioavailability and high toxicity and because of these factors may not affect an intracellular form of the parasite.[62] Therefore, it is crucial to search for new drugs that are effective. Some studies show silver as a treatment of choice due to its antimicrobial properties; however, due to its known cytotoxicity, its application is limited.[63] One way around this problem is to use silver in the form of nanoparticles, because in this formulation it is possible to use smaller doses of the element, thus making it less toxic. Moreover, the use of silver nanoparticles with polysaccharides becomes interesting because many of these molecules can easily cross the cell membrane without causing damage to normal cells.[37,64]

Figure 6 shows the antiparasitic activity of NX when incubated at concentrations of 2.5, 10 and 100 μg/mL for 24 and 48 hrs. BNZ was used as a positive control, as shown in Figure 5. In 24 hrs, only the highest concentration evaluated (100 μg/mL) of BNZ was able to decrease the ability of the parasite to reduce MTT. However, this BNZ effect on parasites decreased after 48 hrs (Figure 5B). This decrease in the effect of BNZ on the parasites in strain Y has also been reported by other authors.[65]

Under no conditions was the xylan able to inhibit the parasite-reducing action against MTT, even with the highest concentration tested (100 μg/mL). A similar result was

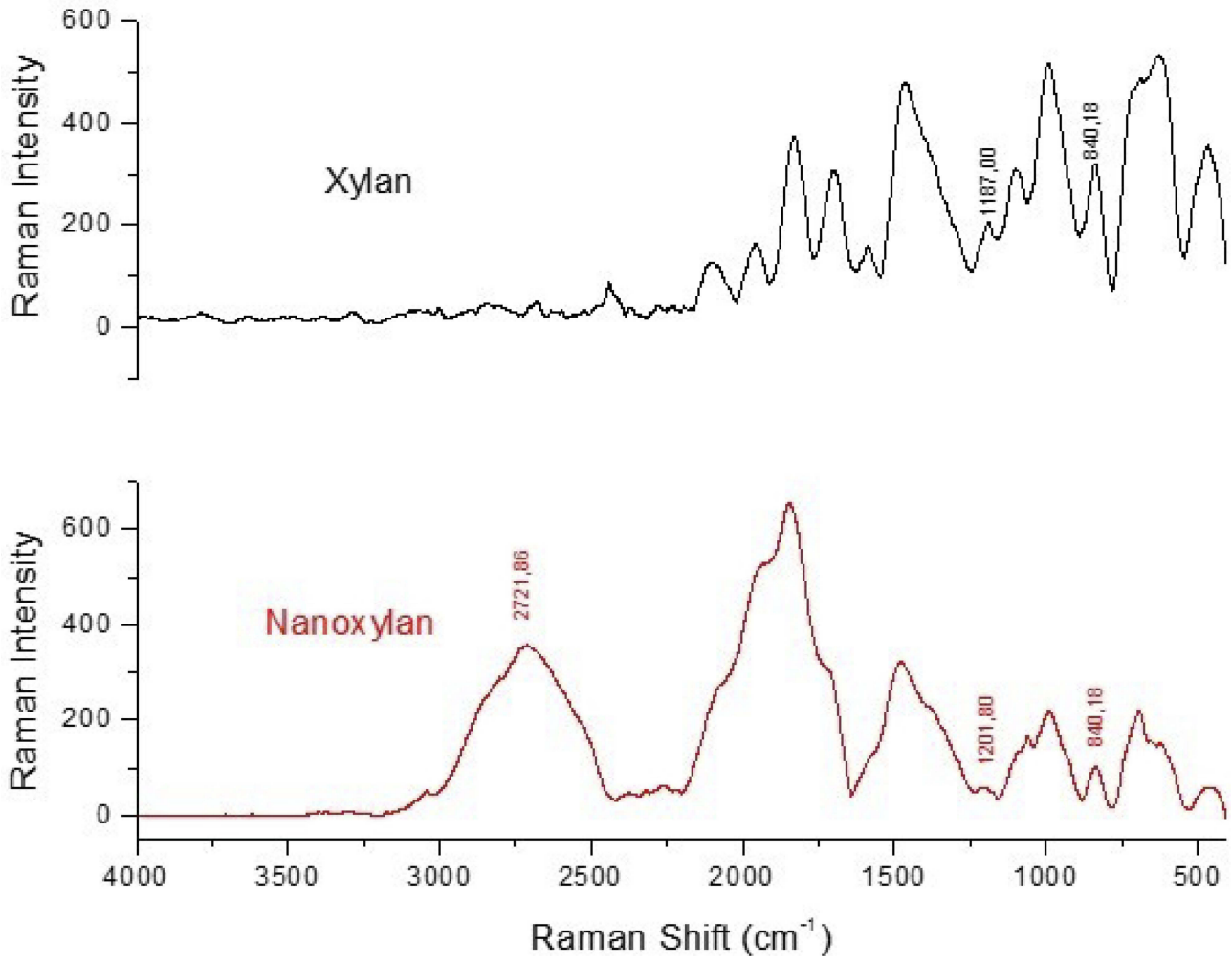

Figure 5 Raman and infrared spectra of xylan and nano xylan.

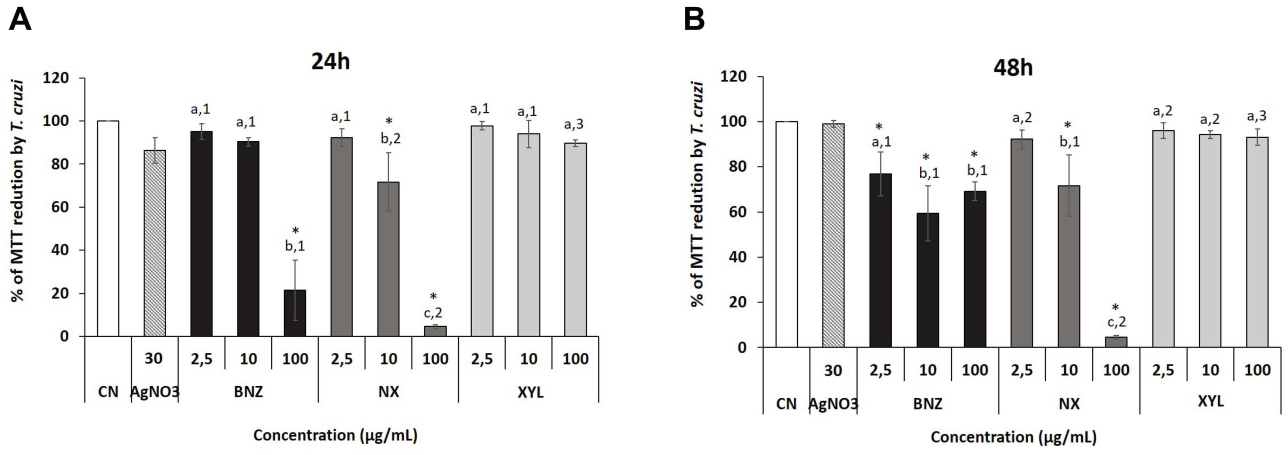

Figure 6 Antiparasitic activity of xylan and nano xylan on the epimastigote forms of *T. cruzi* after incubation for 24 hrs (**A**) and 48 hrs (**B**). The negative control is represented by CN. The positive control (BNZ) is represented by BNZ. Silver nitrate ($AgNO_3$ - 30 µg/mL) and xylan (XYL). Different letters (a, b, c) indicate a significant difference ($p < 0.05$) between various concentrations of the same sample. Different numbers (1, 2, 3) indicate a significant difference ($p < 0.05$) between the same concentration of different samples. * indicates a significant difference ($p< 0.05$) between the negative control (CN) and the different samples. Statistical analysis was performed using ANOVA followed by the Student-Newman-Keuls post-test.

observed when the effect of silver nitrate was evaluated, which showed that xylan and silver, when isolated, do not affect the parasites. It is noteworthy that the amount of silver nitrate used contained 30 µg/mL of silver, which is 1.5 times greater than that present in the 100 µg/mL of NX.

When parasites were exposed to the highest concentration of NX (100 µg/mL), the reduction of MTT by the parasite decreased significantly (82% to 95%, 24 and 48 hrs, respectively) in comparison with the negative control.

When NX cytotoxic activity was evaluated with RAW and 3T3 cells, NX had no toxic effect on cells even at the highest concentration (1 mg/mL) (Data not shown).

For the first time a research group has demonstrated the antiparasitic activity of silver nanoparticles with xylan against the *T. cruzi* protozoan. Although the mechanism of silver nanoparticles has not been properly elucidated, several studies have proposed that the nanoparticles can adhere to the surface of the cell membrane and alter the transmembrane permeability,[66] which may justify the significant decrease in MTT reduction in *T. cruzi*. Therefore, it is believed that the mode of action of NX the same, and this possibility can be confirmed in future studies.

Evaluation of the Process of Cell Death by Annexin V-FITC and PI Labeling

To examine whether data observed in the MTT test were correlated to cell death, the Annexin-V-FITC and PI labeling assay was performed, which differentiates apoptotic, necrotic and viable cells according to the labeling pattern. Strains of *T. cruzi* were treated with NX at concentrations of 2.5, 10 and 100 µg/mL and analysed by flow cytometry. In Figure 7 for the control group, 95.1% of the cells are negative for Annexin V-FITC and PI labeling.

No cell death was observed when lower concentrations of NX were used (2.5 and 10 µg/mL). However, a considerable increase in the percentage of PI-positive cells was found in the treatment that used NX at a concentration of 100 µg/mL (98%), thus demonstrating cell death by necrosis. This fluorochrome has been widely used to determine the necrotic potential of different substances, since it has the characteristic of marking the DNA of cells with membrane damage.[67] Other compounds, such as MBHA3 (3-Hydroxy-2-methylene-3-(4-nitrophenylpropanenitrile)), kill *T. cruzi* by inducing necrosis in which extensive damages to the mitochondrial and plasma membranes are promoted.[68]

Conclusions

The analyses confirmed that a xylan was obtained from the corn cobs. Using this xylan, it was possible to synthesize spherical-shaped silver nanoparticles (nanoxylans) containing 81% xylan and 19% silver. This nanoparticle was able of causing death of the Y strain of the trypanosome *T. cruzi* by the mechanism of necrosis, whereas silver (30 µg/mL) or xylan (100 µg/mL) were not able to. The data described here point to the use of nanoxylans as a possible therapeutic alternative for the treatment of Chagas disease, which can be proven by conducting in vivo studies in the future.

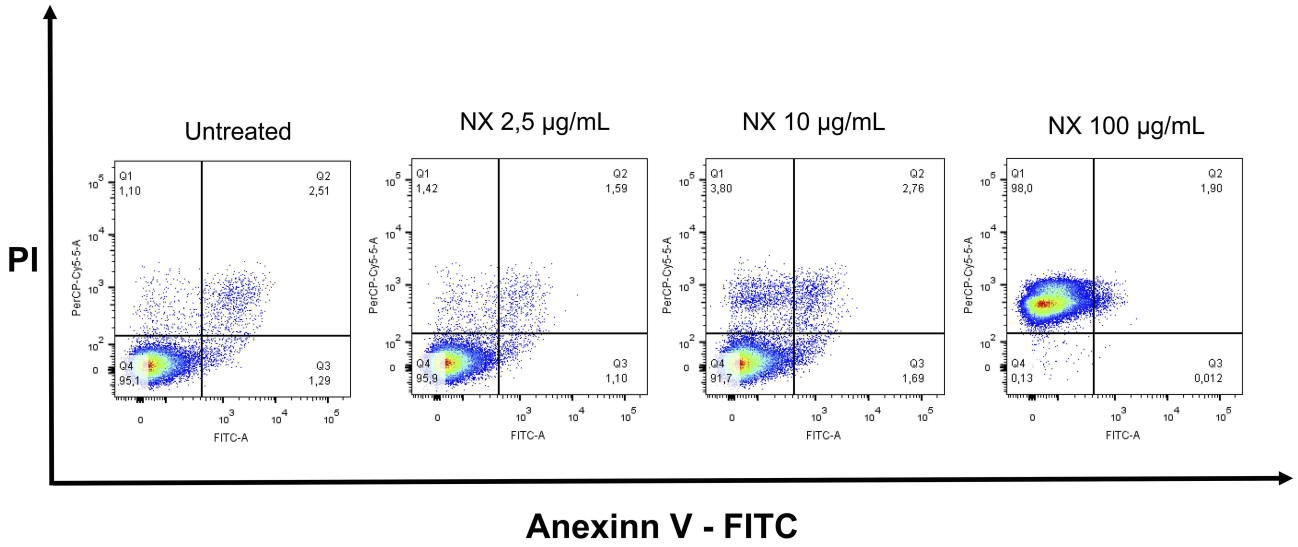

Figure 7 Evaluation of the process of cell death through flow cytometry using untreated parasites, and those treated with (NX) at concentrations of 2.5, 10 and 100 µg/mL for 24 hrs. After this period, the *T. cruzi* parasites were labeled with Annexin V-FITC and Propidium iodide (PI) and analysed using flow cytometry.

Abbreviations

BNZ, Benznidazole; FTIR, Fourier-transform infrared spectroscopy; MTT, 3-bromo (4,5-dimethylthiazol-2-yl)-2,5-diphenyltetrazolium; NX, nano xylan; UV visible, ultraviolet; *T. cruzi, Trypanosoma cruzi*; AFM, Atomic force microscopy; ICP-OES, coupled plasma optical emission spectroscopy; Xyl, xylose; Glc, glucose; Ara, arabinose; Gal, galactose; Man, mannose; GlucA, glucuronic acid; CN, negative control; XYL, xylan; PI, propidium iodide; EDS, energy dispersive X-ray spectroscopy; DLS, dynamic light scattering; SEM, Scanning electron microscopy.

Acknowledgments

The authors wish to thank Conselho Nacional de Desenvolvimento Científico e Tecnológico-CNPq, Coordenação de Aperfeiçoamento Pessoal de Nível Superior-CAPES and Ministério de Ciência, Tecnologia, Informação e Comércio – MCTIC for the financial support. Hugo Rocha is CNPq fellowship honored researchers. To the Department of Biochemistry of the UFRN for providing the flow cytometer where the experiments presented in this paper were performed.

Disclosure

Rony Viana and Mayara Medeiros received a MSc. scholarship from CAPES, and Claudia Moreno had a Ph.D. scholarship from CAPES. This research was submitted to the Graduate Program in Ciências da Saúde (Health Sciences – loose translation) at UFRN, as part of the doctoral thesis of Talita Katiane de Brito. The authors report no other conflicts of interest in this work.

References

1. Gascon J, Bern C, Pinazo MJ. Chagas disease in Spain, the United States and other non-endemic countries. *Acta Trop*. 2010; 115 (1–2): 22–27. doi:10.1016/j.actatropica.2009.07.019
2. Moncayo Á, Silveira AC. Current epidemiological trends for Chagas disease in Latin America and future challenges in epidemiology, surveillance and health policyfile. *Mem Inst Oswaldo Cruz*. 2009;104 (SUPPL. 1):17–30. doi:10.1590/S0074-02762009000900005
3. Schmunis GA, Yadon ZE. Chagas disease: A Latin American health problem becoming a world health problem. *Acta Trop*. 2010; 115 (1–2): 14–21. doi:10.1016/j.actatropica.2009.11.003
4. Pan American Health Organization. Chagas Disease in the Americas: A Review of the Current Public Health Situation and a Vision for the Future. https://www.paho.org/hq/index.php?option=com_docman&view=download&category_slug=technical-reports-3829&alias=45143-chagas-disease-americas-a-review-current-public-health-situation-a-vision-for-future-report-conclusions-recommendations-2018-143&Itemid=270&. Published 2018. Accessed March 18, 2019.
5. World Health Organization. Chagas Disease (American Trypanosomiasis). https://www.who.int/chagas/disease/en/. Published 2018. Accessed January 23, 2019.
6. Salomao K, Menna-Barreto RFS, de Castro SL. Stairway to Heaven or Hell? Perspectives and Limitations of Chagas Disease Chemotherapy. *Curr Top Med Chem*. 2016;16(20):2266–2289. doi:10.2174/1568026616666160413125049
7. Salomão K, et al. *Trypanosoma cruzi* mitochondrial swelling and membrane potential collapse as primary evidence of the mode of action of naphthoquinone analogues. *BMC Microbiol*. 2013;13 (1):196. doi:10.1186/1471-2180-13-196
8. Annang F, Pérez-Moreno G, García-Hernández R, et al. High-Throughput Screening Platform for Natural Product-Based Drug Discovery Against Neglected Tropical Diseases. *J Biomol Screen*. 2014;20(1):82–91. doi:10.1177/1087057114555846
9. Izumi E, et al. Natural products and Chagas' disease: A review of plant compounds studied for activity against *Trypanosoma cruzi*. *Nat Prod Rep*. 2011;28(4):809–823. doi:10.1039/c0np00069h
10. Scotti L, Ferreira EI, Da Silva MS, Scotti MT. Chemometric studies on natural products as potential inhibitors of the nadh oxidase from *Trypanosoma cruzi* using the volsurf approach. *Molecules*. 2010;15 (10):7363–7377. doi:10.3390/molecules15107363
11. Uchiyama N. Antichagasic Activities of Natural Products against *Trypanosoma cruzi*. *J Heal Sci*. 2009;55(1):31–39. doi:10.1248/jhs.55.31
12. Rennie EA, Scheller HV. Xylan biosynthesis. *Curr Opin Biotechnol*. 2014;26:100–107. doi:10.1016/j.copbio.2013.11.013
13. Petzold-Welcke K, Schwikal K, Daus S, Heinze T. Xylan derivatives and their application potential – Mini-review of own results. *Carbohydr Polym*. 2012;100:80–88. doi:10.1016/j.carbpol.2012.11.052
14. Wang Y, et al. Fabrication of optically transparent and strong nanopaper from cellulose nanofibril based on corn cob residues. *Carbohydr Polym*. 2019;214:159–166. doi:10.1016/j.carbpol.2019.03.035
15. Bouramtane S, Bretin L, Pinon A, et al. Porphyrin-xylan-coated silica nanoparticles for anticancer photodynamic therapy. *Carbohydr Polym*. 2019;213:168–175. doi:10.1016/j.carbpol.2019.02.070
16. Kayserilioğlu BŞ, Bakir U, Yilmaz L, Akkaş N. Use of xylan, an agricultural by-product, in wheat gluten based biodegradable films: Mechanical, solubility and water vapor transfer rate properties. *Bioresour Technol*. 2003;87(3):239–246. doi:10.1016/S0960-8524(02)00258-4
17. Nagashima T, Oliveira EE, da Silva AE, et al. Influence of the Lipophilic External Phase Composition on the Preparation and Characterization of Xylan Microcapsules - A Technical Note. *AAPS PharmSciTech*. 2008;9(3):814–817. doi:10.1208/s12249-008-9115-z
18. Yang R, Xu S, Wang Z, Yang W. Aqueous extraction of corn cob xylan and production of xylooligosaccharides. *LWT – Food Sci Technol*. 2005;38(6):677–682. doi:10.1016/j.lwt.2004.07.023
19. Garcia RB, Ganter JLMS, Carvalho RR. D -xylans from corn cobs. *Eur Polym J*. 2000;36:783–787.
20. Oliveira EE, Silva AE, Júnior TN, et al. Xylan from corn cobs, a promising polymer for drug delivery: Production and characterization. *Bioresour Technol*. 2010;101:5402–5406. doi:10.1016/j.biortech.2010.01.137
21. Ebringerová A, Hromádková Z, Hřibalová V. Structure and mitogenic activities of corn cob heteroxylans. *Int J Biol Macromol*. 1995;17:327–331. doi:10.1016/0141-8130(96)81840-X
22. Melo-Silveira RF, Fidelis GP, Pereira Costa MSS, et al. In vitro antioxidant, anticoagulant and antimicrobial activity and in inhibition of cancer cell proliferation by xylan extracted from corn cobs. *Int J Mol Sci*. 2012;13:409–426. doi:10.3390/ijms13010409
23. Morilla MJ, Romero EL. Nanomedicines against Chagas disease: an update on therapeutics, prophylaxis and diagnosis. *Nanomedicine (Lond.)*. 2015; 10(3): 465–481. doi: 10.2217/NNM.14.185
24. Rahul S, Chandrashekhar P, Hemant B, et al. In vitro antiparasitic activity of microbial pigments and their combination with phyto-synthesized metal nanoparticles. *Parasitol Int*. 2015; 64(5): 353–356. doi: 10.1016/j.parint.2015.05.004.

25 Benelli G. Gold nanoparticles – against parasites and insect vectors. *Acta Trop*. 2018; 178: 73–80. doi: 10.1016/j.actatropica.2017.10.021.
26 Burdușel A-C, Gherasim O, et al. Biomedical Applications of Silver Nanoparticles: An Up-to-Date Overview. *Nanomaterials*. 2018;8 (9):681. doi:10.3390/nano8090681
27. Amorim MOR, Lopes Gomes D, Dantas LA, et al. Fucan-coated silver nanoparticles synthesized by a green method induce human renal adenocarcinoma cell death. *Int J Biol Macromol*. 2016;93:57–65. doi:10.1016/j.ijbiomac.2016.08.043
28. Fernandes-Negreiros M, Araújo Machado R, Bezerra F, et al. Antibacterial, Antiproliferative, and Immunomodulatory Activity of Silver Nanoparticles Synthesized with Fucans from the Alga *Dictyota mertensii. Nanomaterials*. 2017;8(1):6. doi:10.3390/nano8010006
29. Melo-Silveira RF, Viana RLS, Sabry DA, et al. Antiproliferative xylan from corn cobs induces apoptosis in tumor cells. *Carbohydr Polym*. 2019;210(November2018): 245–253. doi:10.1016/j.carbpol.2019.01.073
30. Nascimento AKL, Melo-Silveira RF, Dantas-Santos N, et al. Antioxidant and Antiproliferative Activities of Leaf Extracts from *Plukenetia volubilis Linneo (Euphorbiaceae)*. *Evidence-Based Complement Altern Med*. 2013;2013:1-10. doi:10.1155/2013/950272
31. Bradford MM. Sistema séptico domiciliario | Rotomoldeo en Colombia Tanques Plasticos En Colombia Rotoplast. *Anal Biochem*. 1976;72:248–254. doi:10.1016/0003-2697(76)90527-3
32. Dubois M, Gilles KA, Hamilton JK, et al. Colorimetric Method for Determination of Sugars and Related Substances. *Anal Chem*. 1956;28(3):350–356. doi:10.1021/ac60111a017
33. Dipankar C, Murugan S. The green synthesis, characterization and evaluation of the biological activities of silver nanoparticles synthesized from *Iresine herbstii* leaf aqueous extracts. *Colloids Surfaces B Biointerfaces*. 2012;98:112–119. doi:10.1016/j.colsurfb.2012.04.006
34. Kačuráková M, Belton PS, Wilson RH, et al. Hydration properties of xylan-type structures: An FTIR study of xylooligosaccharides. *J Sci Food Agric*. 1998;77:38–44. doi:10.1002/(SICI)1097-0010(199805)77:1<38::AID-JSFA999>3.0.CO;2-5
35. Martinez-Castanon GA, Niño-Martínez N, et al. Synthesis and antibacterial activity of silver nanoparticles with different sizes. *J Nanoparticle Res*. 2008;10(8):1343–1348. doi:10.1007/s11051-008-9428-6
36. Song JY, Jang HK, Kim BS. Biological synthesis of gold nanoparticles using Magnolia kobus and Diopyros kaki leaf extracts. *Process Biochem*. 2009;44(10):1133–1138. doi:10.1016/j.procbio.2009.06.005
37. Pandey S, Goswami GK, Nanda KK. Green synthesis of biopolymer-silver nanoparticle nanocomposite: An optical sensor for ammonia detection. *Int J Biol Macromol*. 2012;51:583–589. doi:10.1016/j.ijbiomac.2012.06.033
38. Chen X, Yan JK, Wu JY. Characterization and antibacterial activity of silver nanoparticles prepared with a fungal exopolysaccharide in water. *Food Hydrocoll*. 2016;53:69–74. doi:10.1016/j.foodhyd.2014.12.032
39. Silva LP, Bonatto CC, Pereira FDES, et al. Nanotecnologia verde para síntese de nanopartículas metálicas. *Biotecnol Apl à Agro&Indústria* - Vol 4. 2017: 967–1012. doi:10.5151/9788521211150-26
40. Kato H, Suzuki M, Fujita K et al. Reliable size determination of nanoparticles using dynamic light scattering method for in vitro toxicology assessment. *Toxicol. In Vitro* 2009; 23:927–934. doi: 10.1016/j.tiv.2009.04.006.
41. Bhatterjee, S. DLS and zeta potential –What they are what they are not? *J. Control. Release* 2016; 235:337–351. doi: 10.1016/j.jconrel.2016.06.017.
42. Nel A. Toxic Potential of Materials at the Nanolevel. *Science* (80-). 2006;311(5761):622-627. doi:10.1126/science.1114397
43. Carlson C, Hussein SM, Schrand AM, et al. Unique cellular interaction of silver nanoparticles: Size-dependent generation of reactive oxygen species. *J Phys Chem B*. 2008;112(43):13608–13619. doi:10.1021/jp712087m
44. Liu W, Wu Y, Wang C, et al. Impact of silver nanoparticles on human cells: Effect of particle size. *Nanotoxicology*. 2010;4(3):319–330. doi:10.3109/17435390.2010.483745
45. Akter M, Sikder MT, Rahman MM, et al. A systematic review on silver nanoparticles-induced cytotoxicity: Physicochemical properties and perspectives. *J Adv Res*. 2018;9:1–16. doi:10.1016/j.jare.2017.10.008
46. Stoehr LC, Gonzalez E, Stampfl A, et al. Shape matters: Effects of silver nanospheres and wires on human alveolar epithelial cells. *Part Fibre Toxicol*. 2011;8(1):36. doi:10.1186/1743-8977-8-36
47. Kumar S, Negi YS. Corn cob xylan-based nanoparticles: Ester prodrug of 5-aminosalicylic acid for possible targeted delivery of drug. *J Pharm Sci Res*. 2012;4:1995–2003.
48. Sun JL, Sakka K, Karita S, et al. Adsorption of *Clostridium stercorarium* xylanase A to insoluble xylan and the importance of the CBDs to xylan hydrolysis. *J Ferment Bioeng*. 1998;85(1):63–68. doi:10.1016/S0922-338X(97)80355-8
49. Colom X, Carrillo F, Nogués F, Garriga P. Structural analysis of photodegraded wood by means of FTIR spectroscopy. *Polym Degrad Stab*. 2003;80(3):543–549. doi:10.1016/S0141-3910(03)00051-X
50. Sun XF, Xu F, Sun RC, et al. Characteristics of degraded hemicellulosic polymers obtained from steam exploded wheat straw. *Carbohydr Polym*. 2005;60(1):15–26. doi:10.1016/j.carbpol.2004.11.012
51. Li C. Exploring C – C Bond Formations beyond. Accounts. 2009;42 (2):335–344.
52. Nacos MK, Katapodis P, Pappas C, et al. Kenaf xylan – A source of biologically active acidic oligosaccharides. *Carbohydr Polym*. 2006;66(1):126–134. doi:10.1016/j.carbpol.2006.02.032
53. Barroso EMA, Costa LS, Medeiros VP, et al. A non-anticoagulant heterofucan has antithrombotic activity in vivo. *Planta Med*. 2008;74 (7):712–718. doi:10.1055/s-2008-1074522
54. Luo Y, Shen S, Luo J, et al. Green synthesis of silver nanoparticles in xylan solution via Tollens reaction and their detection for Hg2+. *Nanoscale*. 2015;7:690–700. doi:10.1039/c4nr05999a
55. He Y, Du, Tang, et al. Green synthesis of silver nanoparticles by *Chrysanthemum morifolium* Ramat. extract and their application in clinical ultrasound gel. *Int J Nanomedicine*. 2013;8:1809. doi:10.2147/IJN.S43289
56. Christophe F, Séné B, et al. Fourier-Transform Raman and Fourier-Transform lnfrared Spectroscopy. *Plant Physiol*. 1994;106:1623–1631.
57. Zeng Y, Yarbrough JM, Mittal A, et al. In situ label-free imaging of hemicellulose in plant cell walls using stimulated Raman scattering microscopy. *Biotechnol Biofuels*. 2016;9:256. doi:10.1186/s13068-016-0669-9
58. Barron C, Robert P, Guillon F, et al. Structural heterogeneity of wheat arabinoxylans revealed by Raman spectroscopy. *Carbohydr Res*. 2006. doi:10.1016/j.carres.2006.03.025
59. Cao Y, Shen D, et al. A Raman-scattering study on the net orientation of biomacromolecules in the outer epidermal walls of mature wheat stems (*Triticum aestivum*). *Handb Environ Chem Vol 5 Water Pollut*. 2006;97:1091–1094. doi:10.1093/aob/mcl059
60. Li JF, Zhang YJ, et al. Core-shell nanoparticle-enhanced Raman spectroscopy. *Chem Rev*. 2017;117(7):5002–5069. doi:10.1021/acs.chemrev.6b00596
61. Akmaz S., Adıgüzel E.D., et al. The Effect of Ag Content of the Chitosan-Silver Nanoparticle Composite Material on the Structure and Antibacterial Activity. *Adv Mater Sci Eng*. 2013:6. doi:http://dx.doi.org/10.1155/2013/690918
62. Lamas MC, Villaggi L, Nocito I, et al. Development of parenteral formulations and evaluation of the biological activity of the trypanocide drug benznidazole. *Int J Pharm*. 2006;307(2):239–243. doi:10.1016/j.ijpharm.2005.10.004

63. Rai M, Yadav A, Gade A. Silver nanoparticles as a new generation of antimicrobials. *Biotechnol Adv*. 2009;27(1):76–83. doi:10.1016/j.biotechadv.2008.09.002
64. Pal S, Tak YK, Song JM. Does the antibacterial activity of silver nanoparticles depend on the shape of the nanoparticle? A study of the gram-negative bacterium *Escherichia coli*. *J Biol Chem*. 2015. doi:10.1128/AEM.02218-06
65. Muelas-Serrano S, Nogal-Ruiz JJ, Gómez-Barrio A. Setting of a colorimetric method to determine the viability of *Trypanosoma cruzi* epimastigotes. *Parasitol Res*. 2000;86:999–1002. doi:10.1007/PL00008532
66. Sharma VK, Yngard RA, Lin Y. Silver nanoparticles: Green synthesis and their antimicrobial activities. *Adv Colloid Interface Sci*. 2009;145:83–96. doi:10.1016/j.cis.2008.09.002
67. Kumar SP, Birundha K, et al. Antioxidant studies of chitosan nanoparticles containing naringenin and their cytotoxicity effects in lung cancer cells. *Int J Biol Macromol*. 2015;78:87–95. doi:10.1016/j.ijbiomac.2015.03.045
68. Sandes JM, Borges AR, Junior CGL, et al. 3-Hydroxy-2-methylene-3-(4-nitrophenylpropanenitrile): A new highly active compound against epimastigote and trypomastigote form of *Trypanosoma cruzi*. *Bioorg Chem*. 2010;38(5):190–195. doi:10.1016/j.bioorg.2010.06.003